

Supplementary Information

Cooperation of local motions in the Hsp90 molecular chaperone ATPase mechanism

**Andrea Schulze¹, Gerti Beliu¹, Dominic A. Helmerich¹, Jonathan Schubert¹,
Laurence H. Pearl², Chrisostomos Prodromou² & Hannes Neuweiler^{1,*}**

¹Department of Biotechnology and Biophysics, Julius-Maximilians-University Würzburg,
Am Hubland, 97074 Würzburg, Germany

²Genome Damage and Stability Centre, School of Life Sciences, University of Sussex,
Falmer, Brighton BN1 9RQ, United Kingdom

*Corresponding author: hannes.neuweiler@uni-wuerzburg.de

Supplementary Results

Supplementary Tables

Table 1: Kinetic parameters of local motions of Hsp90 measured at 25°C.

Mutant	Reporter	a_1^a	k_1^a	a_2^a	k_2^a	a_3^a	k_3^a	mean k^b
Wild type	β -Strand swap	0.59 ± 0.07	0.31 ± 0.02	0.19 ± 0.02	0.05 ± 0.005	0.22 ± 0.03	1.47 ± 0.24	0.18 ± 0.01
Wild type	N/M association	0.68 ± 0.05	0.41 ± 0.03	0.32 ± 0.008	0.08 ± 0.007			0.18 ± 0.02
Wild type	Lid closure	0.55 ± 0.01	0.33 ± 0.01	0.45 ± 0.007	0.10 ± 0.002			0.16 ± 0.003
A2W-L160W	β -Strand swap ^c	0.35 ± 0.07	0.10 ± 0.01	0.65 ± 0.04	0.02 ± 0.001			0.03 ± 0.0005
A2W-L160W	N/M association	0.72 ± 0.04	0.20 ± 0.01	0.28 ± 0.04	0.04 ± 0.004			0.10 ± 0.01
A2W-L160W	Lid closure	0.5 ± 0.03	0.14 ± 0.01	0.5 ± 0.07	0.05 ± 0.002			0.07 ± 0.0005
A107N	β -Strand swap	0.61 ± 0.05	2.47 ± 0.37	0.27 ± 0.05	0.62 ± 0.10	0.12 ± 0.03	0.05 ± 0.01	0.34 ± 0.03
A107N	N/M association	0.84 ± 0.02	1.63 ± 0.05	0.16 ± 0.02	0.20 ± 0.04			0.78 ± 0.06
A107N	Lid closure	0.32 ± 0.09	0.40 ± 0.08	0.68 ± 0.14	1.37 ± 0.21			0.79 ± 0.08

^a a_n and k_n are the relative fluorescence amplitudes and observed rate constants ($1/\tau_n$ in 1/min). Data represent mean values \pm s.d. of three measurements.

^b The mean rate constant was calculated from the sum of individual time constants weighted by the respective amplitudes ($1/(\sum a_n \tau_n)$).

^c To monitor domain swap of the TrpZip mutant A2W-L160W, the fluorophore was placed in waiting position on the second subunit of heterodimeric Hsp90 (E162C).

Table 2: ATPase activity of wild-type Hsp90 and mutants thereof measured at 37°C.

Mutant	ATPase (min^{-1})
Wild type	1.6 \pm 0.04
A2W-L160W	0.61 \pm 0.09
T101I	0.35 \pm 0.06
F349A	0.12 \pm 0.02
R380A	ND

ND; not detectable; data represent mean values \pm s.d. of three measurements.

Table 3: Kinetics of local motions of wild-type Hsp90 in the presence of Aha1 measured at 25 °C.

Mutant	Reporter + Aha1	a_1^a	k_1^a	a_2^a	k_2^a	mean k^b		
Wild type	β -Strand swap	0.59±0.06	35.3±3.0	0.41±0.06	1.8±0.27	4.2±0.25		
Wild type	N/M association	0.80±0.01	18.4±0.97	0.20±0.01	2.1±0.03	7.2±0.5		
Wild type	Lid closure	0.52±0.04	10.5±2.2	0.48±0.04	2.1±0.4	3.6±0.55		
F349A	β -Strand swap	0.62±0.08	2.84±0.22	0.28±0.1	0.49±0.002	0.1±0.02	0.05±0.01	0.31±0.06
F349A	N/M association	0.70±0.15	0.94±0.41	0.3±0.07	0.15±0.03	0.35±0.08		
F349A	Lid closure	ND	ND	ND	ND	ND		

^a a_n and k_n are the relative fluorescence amplitudes and observed rate constants ($1/\tau_n$ in 1/min). Data represent mean values \pm s.d. of three measurements.

^b The mean rate constant was calculated from the sum of individual time constants weighted by the respective amplitudes ($1/(\sum a_n \tau_n)$).

ND; not detectable.

Table 4: Dynamics of NTD structural elements measured by PET-FCS at 25 °C

N-terminal domain	a₁	τ₁ (μs)	a₂	τ₂ (μs)	a₃	τ₃ (μs)
Q14C-A2W	0.67±0.06	392±23	0.10±0.01	6±3	--	--
Q14C-A2W +ATP	0.53±0.02	429±36	0.08±0.01	11±10		
Q14C-A2W-L160W	--	--	--	--	--	--
A112C-S25W	0.78±0.01	375±18	0.14±0.01	7±2	--	--
A112C-S25W + ATP	0.29±0.01	300±4	0.15±0.01	7±1		
NM-domain						
Q14C-A2W	1.03±0.09	940±140	0.59±0.12	145±38	0.15±0.03	0.9±0.8
Q14C-A2W +ATP	0.89±0.03	882±79	0.42±0.06	130±24	0.18±0.05	0.3±0.1
Q14C-A2W +Aha1	0.92±0.03	1000±100	0.61±0.07	170±20	0.15±0.08	1.9±0.8
A112C-S25W	0.56±0.02	350±40	0.26±0.01	15±7	0.27±0.05	0.5±0.4
A112C-S25W + ATP	0.20±0.01	233±13	0.19±0.01	11±1	0.21±0.05	0.2±0.1
A112C-S25W + Aha1	0.17±0.01	157±20	0.20±0.01	7±1	0.45±0.14	0.2±0.1

a_n and τ_n are the observed amplitudes and corresponding time constants. Data represent mean values ± s.d. of three measurements.

Supplementary Figures

Figure 1

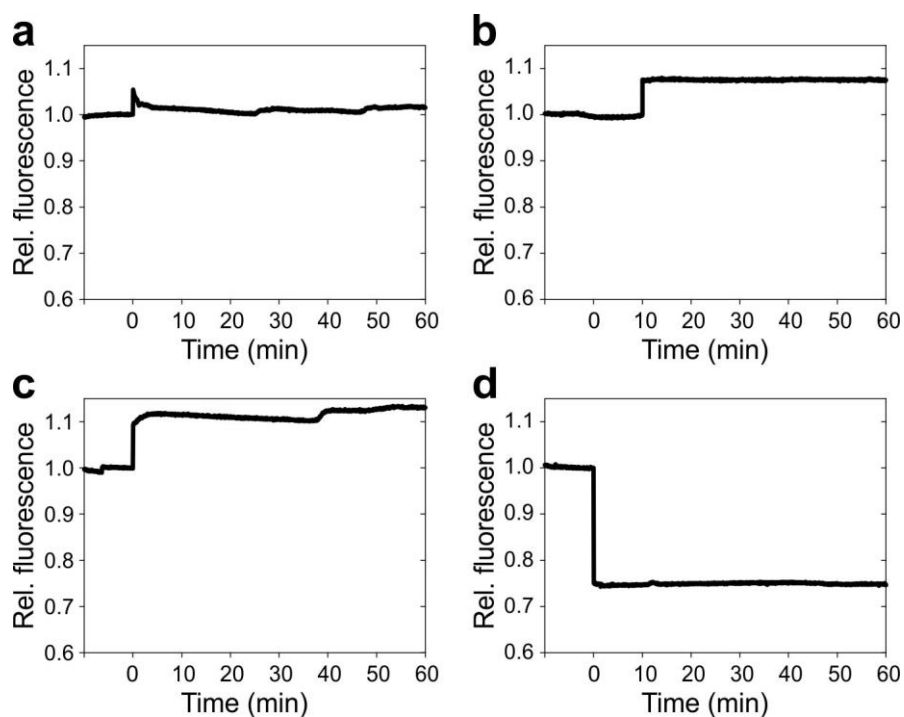


Figure 1: Influence of ADP on conformational switches of Hsp90

Fluorescence intensity time traces measured for (a) β -strand swap (A2C+E162W), (b) N/M-domain association (E192C-N298W), and (c)/(d) lid closure (reporters S51C-A110W and S51W-A110C, respectively). 4 mM ADP was added at time $t = 0$ min. Measurements were done at 25°C.

Figure 2

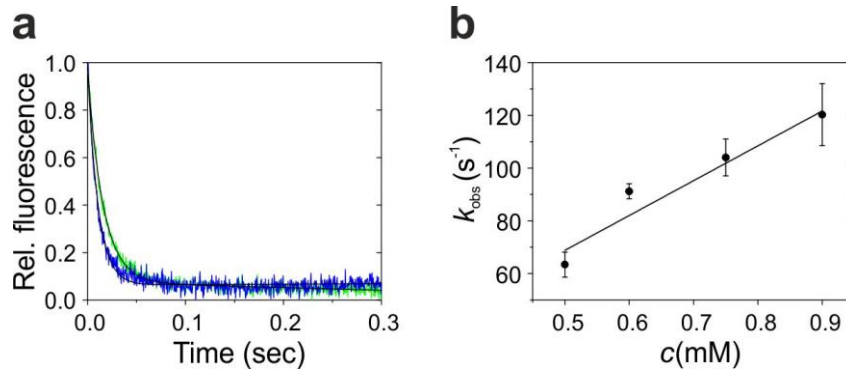


Figure 2: Kinetics of early remodeling of the lid induced by binding of nucleotide

(a) Representative fluorescence intensity time traces of reporter S51W-A110C on Hsp90 measured using stopped-flow fluorescence spectroscopy. Kinetic transients were triggered by binding of 0.5 mM ADP (green) and 0.75 mM ADP (blue). Each time trace is an average over three individual shots. Black lines are single exponential fits to the data. We used ADP instead of ATP to solely trigger remodeling of the lid and to avoid possible interference from other conformational changes that could complicate data analysis. (b) Observed rate constants plotted versus concentration of ADP. Data represent mean values \pm s.d. of three measurements (performed at 25 °C). The black line is a linear fit to the data that yielded a bi-molecular rate constant of $1.3 \pm 0.2 \times 10^5 \text{ M}^{-1} \text{ s}^{-1}$.

Figure 3

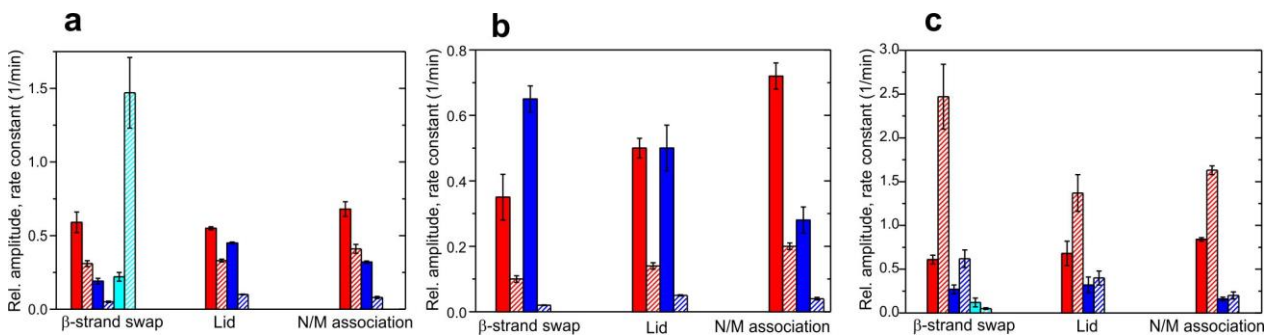


Figure 3: Heterogeneity of kinetics of conformational switching

Plot of the observed amplitudes and rate constants of the individual exponential phases in multi-exponential decays of conformational switching (see Supplementary Table 1). Amplitudes (filled bars) and corresponding rate constants (patterned bars) are shown in same color. Panels (a), (b), and (c), show kinetics measured for wild-type Hsp90, the TrpZip construct, and mutant A107N, respectively. Data represent mean values \pm s.d. of three measurements.

Figure 4

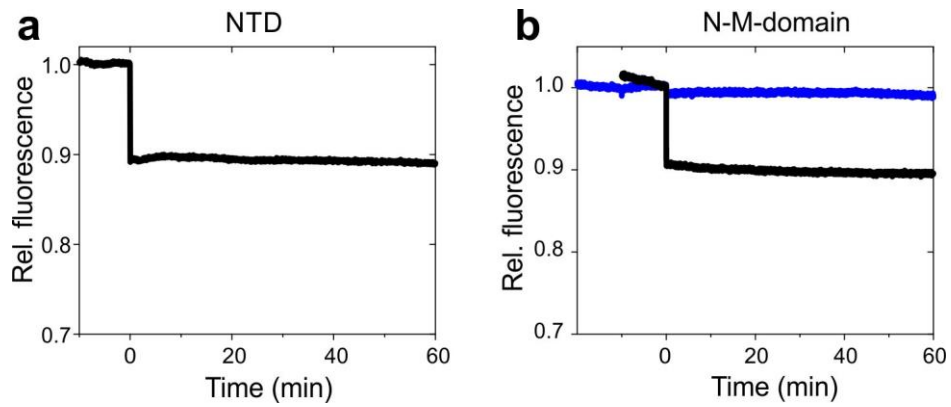


Figure 4: Influence of binding of AMP-PNP on motion of the lid in isolated NTD and NM-domain.

(a) Fluorescence intensity time traces measured for reporter A110C-S51W on the NTD in isolation, which probes closure of the lid. 2 mM AMP-PNP was added at time $t = 0$ min. (b) The same measurement for reporter S51C-A110W on the NM-domain in absence (black) and presence (blue) of 20 μ M Aha1. Aha1 was added at $t = -10$ min and AMP-PNP at $t = 0$ min. Measurements were done at 25°C.

Figure 5

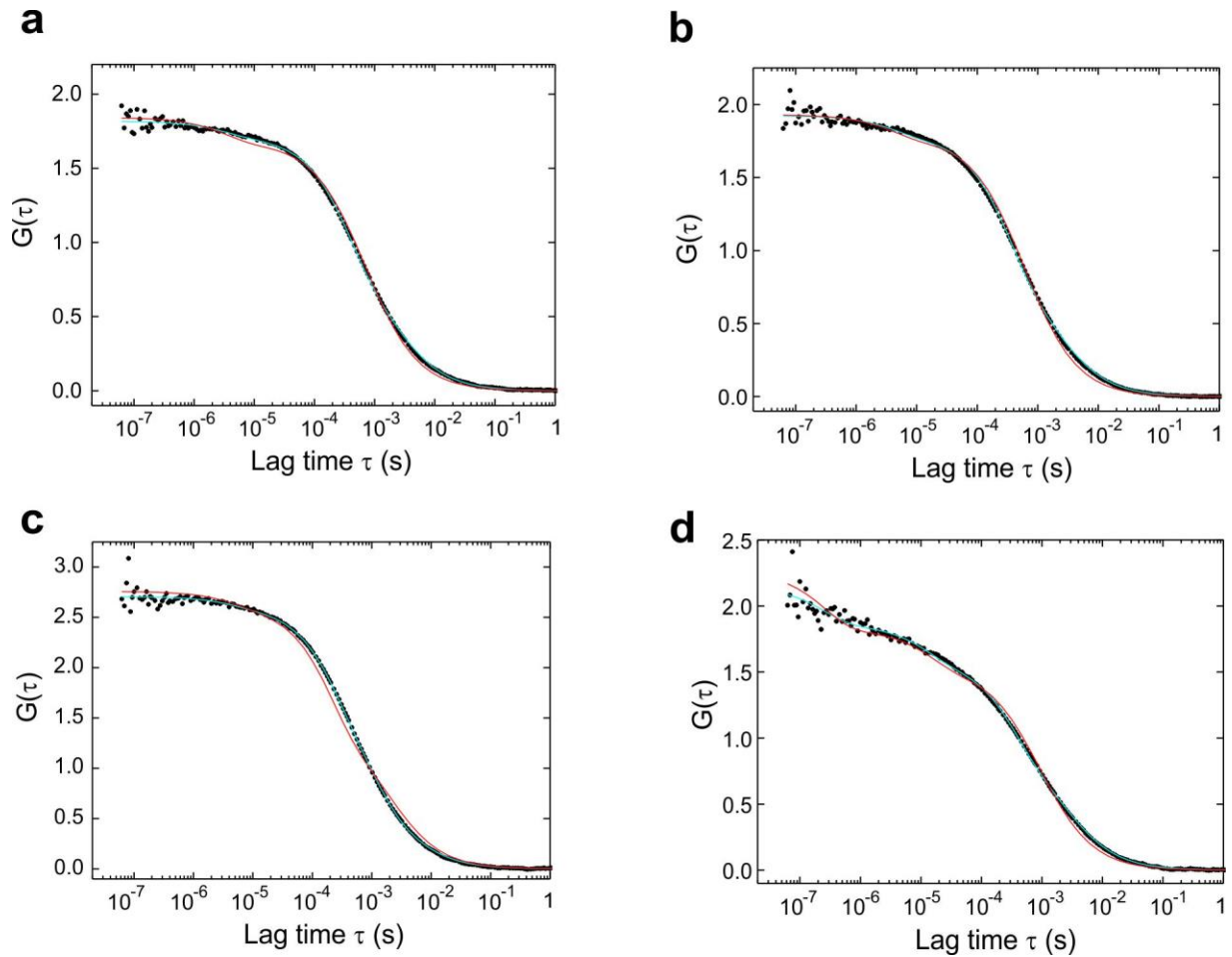


Figure 5: Analysis of PET-FCS data using a model that lacks a 300-900 μs exponential relaxation.

(a), (b) ACFs recorded from β -strand reporter Q14C-A2W and from lid reporter A112C-S25W, respectively, on the isolated NTD. (c), (d) ACFs recorded from β -strand reporter Q14C-A2W and from lid reporter A112C-S25W, respectively, on the NM-domain. In case of the NTD ((a) and (b)), cyan lines are fits to the data using a model for molecular diffusion containing two single-exponential relaxations. In case of the NM-domain ((c) and (d)), cyan lines are fits to the data using a model for molecular diffusion containing three single-exponential relaxations. Red lines are fits to the data using the same models but lacking a single-exponential relaxation at 300-900 μs . These fits yielded artificially small diffusion time constants due to overlap of time scales of diffusion and conformational fluctuations. Specifically, the NTD had a diffusion time constant of 1.7 ms that was artificially reduced to 0.6-0.7 ms. The NM-domain had a diffusion time constant of 2.2 ms that was artificially reduced to 1.9 and 0.9 ms.